PCCP

COMMUNICATION

View Article Online
View Journal | View Issue

Cite this: *Phys. Chem. Chem. Phys.*, 2016, **18**, 18692

Received 4th May 2016,
Accepted 29th June 2016

DOI: 10.1039/c6cp02999j

www.rsc.org/pccp

CO chemisorption at vacancies of supported graphene films: a candidate for a sensor?†

E. Celasco,*[ab] G. Carraro,[ab] A. Lusuan,[ab] M. Smerieri,[b] J. Pal,‡[ab] M. Rocca,[ab] L. Savio[b] and L. Vattuone[ab]

We investigate CO adsorption at single vacancies of graphene supported on Ni(111) and polycrystalline Cu. The borders of the vacancies are chemically inert but, on the reactive Ni(111) substrate, CO intercalation occurs. Adsorbed CO dissociates at 380 K, leading to carbide formation and mending of the vacancies, thus preventing their effectiveness in sensor applications.

Graphene (G) is known to be chemically "inert" in its pristine configuration, *i.e.* in absence of defects,[1] although it can induce complexation reactions by its delocalized π-electron system.[2] Both intercalation and reaction of CO below G have been reported previously.[3–5] Theoretical calculations confirm low adsorption energies for simple molecules on pristine, free standing graphene[6] (8–14 meV for CO, depending on adsorption site), but predict strong bonds at graphene vacancies and at substitutional defects (up to ∼1.7 eV and ∼6.3 eV, respectively).[7–9] Defects affect also the electronic properties of the G layer: a local modification of the density of states has been reported by STS following ion irradiation[10] and opening of the gap occurs for patterned adsorption[11,12] (with a possible influence on the electric response to adsorbates and, consequently, on the sensor properties[13,14]).

The possibility to realize graphene based devices for gas sensing and in particular for detecting CO in concentration of 1 to 100 ppm,[13,14] has been recently reported.

Such devices are based on the fact that CO acts as an electron donor and causes a reproducible increase in the resistance of the graphene film attaining its final value on at time scale of several minutes. The nature of the CO adsorption site remained, however, unexplored. The high exposure required to observe a CO-related signal indicates a low net sticking probability. On the other hand, the need to operate the sensor at 300 °C[15] or to re-generate it by annealing to 150 °C[13] suggests that the active sites have a relatively high adsorption energy, *i.e.* that adsorption occurs at defects. Indeed, we have recently demonstrated that pristine G layers are reactive towards CO only when supported on a strongly interacting substrate such as Ni(111). Also then, CO adsorbs reversibly at room temperature.[16]

To clarify the nature of the adsorption site in the CP adsorption process, we investigated experimentally CO adsorption at defected graphene single layers under Ultra High Vacuum (UHV) conditions and compared their reactivity when grown or deposited on two different substrates: Ni(111) (G/Ni in the following) and polycrystalline Cu (G/Cu). The chemical properties of the films were investigated by X-ray Photoelectron Spectroscopy (XPS) and by High Resolution Electron Energy Loss Spectroscopy (HREELS). For the G/Ni(111) sample also a morphological analysis by STM was performed by repeating the preparation in a dedicated UHV apparatus.

For all samples, vacancies were created by 150 eV Ne^+ ion bombardment at normal incidence for the spectroscopy experiments. On the contrary, ion bombardment was applied ∼55° off normal incidence in the STM experiments for G/Ni(111) due to geometrical constraints of the corresponding apparatus. According to previous experimental[17,18] and theoretical[19] studies, Ne^+ irradiation under very similar conditions produces single and double vacancies (*i.e.* situations in which only one C atom or two adjacent C atoms of the G lattice are removed, respectively) in ∼5 : 2 ratio.

Fig. 1 compares HREEL spectra recorded for different samples before and after exposure to 400 L CO at room temperature (RT). Given the density of C atoms in G (∼3.85×10^{15} atoms per cm^2) in order to produce a low density of isolated vacancies the sputtering dose is $\chi_{Ne^+} = 3.2 \times 10^{14}$ Ne^+/cm^2 for both the G/Ni and the G/Cu samples.

Starting from the G/Ni(111) (Fig. 1A), we can see that before ion bombardment weak losses at 63 meV and 90 meV are present corresponding to defects of graphene[20] and to the

[a] *Dipartimento di Fisica, Università di Genova, 16146 Genova, Italy. E-mail: celasco@fisica.unige.it*
[b] *IMEM-CNR Unità Operativa di Genova, 16146 Genova, Italy*

† Electronic supplementary information (ESI) available: Details of the experimental methods; assignment of the vibrational losses not related to CO in the spectra of Fig. 1B; additional note. See DOI: 10.1039/c6cp02999j

‡ Present address: Department of Chemical Physics, Fritz Haber Institute of the Max Planck Society, Faradayweg 4-6, 14195 Berlin, Germany.

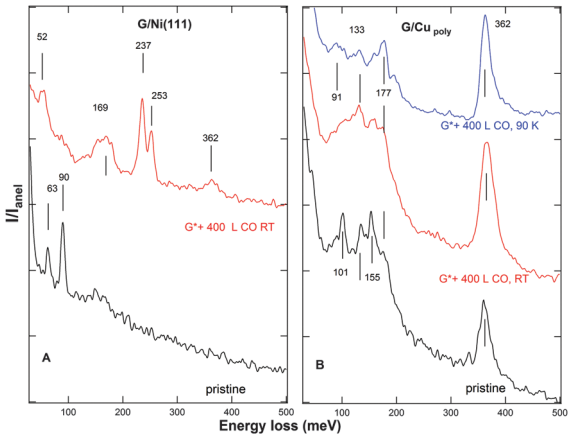

Fig. 1 HREEL spectra recorded in-specular and corresponding to experiments performed for: (A) G on Ni(111), (B) G on polycrystalline Cu and. In each panel the spectra are normalized to the inelastic background I_{anel} between 450 and 500 meV loss energy and are vertically shifted for sake of clarity.

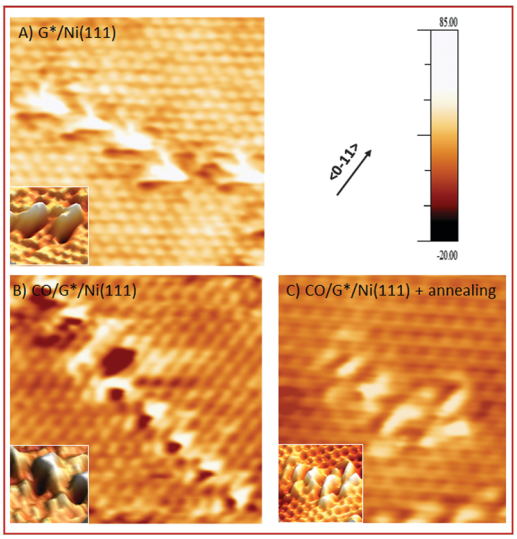

Fig. 2 STM image of (A) G*/Ni(111) without CO exposure (V = 0.05 V, I = 0.6 nA), (B) G*/Ni(111) after 400 L CO exposure (V = −0.02 V, 0.7 nA) and (C) G*/Ni(111) with 400 L CO after annealing to 400 K (V = −0.15 V, 0.7 nA). For all images, size: 35 × 35 nm^2; the same scale, reported in the top-right panel, was employed for the apparent height (in pm). In each panel the inset shows a three dimensional rendering of a small defected area of the corresponding image.

z-polarized phonon,[21] respectively. No vibrational signature of CO adsorption has been observed on the pristine layer exposed at RT under UHV conditions,[16] while additional peaks show up at 52 meV, 237 meV and 253 meV for the ion bombarded graphene layer (indicated as G*). They correspond to the molecule – surface and to the internal C–O stretch mode for bridge and atop configurations, respectively.[22] Their presence proves that CO adsorption has occurred. A further broad peak is visible at about 169 meV, a frequency close to the one of the D band in Raman spectra[23] and which is considered a marker of surface disorder. It is present also for defected samples not exposed to CO (not shown§) so that we assign it to distorted G configurations. The loss at 362 meV corresponds to the C–H stretch resulting from water dissociation.[24]

For G/Cu$_{poly}$ (Fig. 1B), we observe that in the initial spectrum (black) losses are already present at 101 meV, 133 meV, 155 meV, 177 meV and 362 meV. Since the as-delivered sample was introduced into vacuum and treated only by a mild annealing to 390 K, these modes correspond to residual traces of contaminants (in particular the losses at 177 meV and at 362 meV correspond to the presence of CH groups[24]) and to distorted configurations of the graphene layer (see SM for details). Contrary to the case of G*/Ni(111), no additional losses are detected following the exposure to 400 L CO (neither at RT nor at 90 K) indicating that the G* layer on Cu is inert.

The energy of the losses at 52 meV, 237 meV, and 253 meV observed for G*/Ni(111) are close to those reported for CO/Ni(111)[22] at high coverage (50 meV, 237 meV and 254 meV, respectively). The CO stretch frequency is notably lower than the one reported for CO chemisorbed on pristine G/Ni at 90 K.[16,25] This leads to the conclusion that CO reaches the Ni substrate through the vacancies. Since intercalation below G/Pt(111) causes a red-shift of the CO stretch frequency of ∼2 meV[4], we conclude that a high local coverage of CO is reached for G*/Ni(111) when exposed to CO.

The corresponding STM image for G*/Ni(111) (see Fig. 2A) shows localized defects. They are compatible in size with the production of mostly monoatomic vacancies following ion irradiation. Since each hole has a protrusion on its side,[26] it is reasonable that the displaced C atom has ended up above the G* layer close to the defect.

Even if it is not possible to resolve the presence of CO ad-molecules close to or into the graphene vacancies, inspection of a typical image recorded before and after CO dose (panel A and B respectively) shows a change in the apparent shape and dimensions of the defects, indicating that the system is modified by adsorption.

The data reported above clearly indicate that CO adsorption occurs only for G*/Ni(111), *i.e.* in presence of a reactive substrate. Adsorption was investigated as a function of χ_{Ne^+} (sputtering dose) by XPS and HREELS (see Fig. 3). XPS spectra were recorded after sputtering and prior to CO exposure. *Vice versa*, HREEL spectra were recorded after exposing the samples to 400 L CO at RT. We can infer that:

(1) After the mildest sputtering dose (second spectrum from the bottom), the C 1s peak in XPS shifts to lower binding energy while a broad energy loss develops around 169 meV in HREELS. This change is due to the detachment of G from the Ni(111) substrate when vacancies form and when Ne atoms intercalate. Indeed, E_b(C 1s) downshifts towards 284.3 eV, a value close to the one reported in the literature for graphene on Ni(111) "decoupled" by CO intercalation at high pressure.[27] Moreover, at the largest Ne^+ dose (3.2×10^{14} Ne^+/cm^2), a Ne 1s signal is visible at 863 eV as a shoulder of the Ni $2p^{3/2}$ peak, corresponding to a concentration of ∼4% with respect to C. Given the surface density of Ni(111), for this ion dose each C atom has a probability of ∼9% of being hit by one Ne^+ ion during irradiation. Assuming the defect creation probability given in ref. 19,

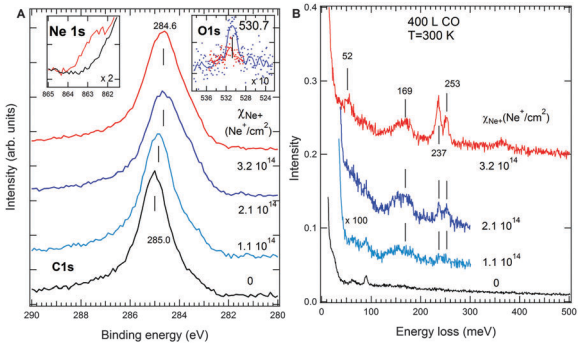

Fig. 3 (A) XPS spectra of the C 1s line following ion bombardment and prior to CO exposure. Inspection of the Ne 1s region after the highest sputtering dose proves intercalation[29] (see left inset; black/red spectrum corresponds to pristine/defected G layer). The inset on the right shows the O 1s signal after 400 L CO following χ_{Ne^+} = 2.1 × 10^{14} Ne^+/cm^2 (blue) and after annealing to 450 K (red). (B) HREEL spectra recorded in-specular and normalized to the elastic intensity, after exposing pristine and ion bombarded G/Ni(111) to 400 L CO at RT.

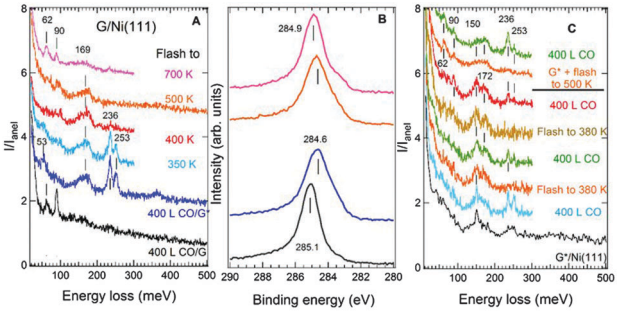

Fig. 4 (A) HREEL spectra recorded in-specular after annealing the CO covered G* layer to different temperatures. (B) XPS spectra for pristine G/Ni(111) (black), CO covered G*/Ni following 3.2 × 10^{14} Ne^+ irradiation (blue) and after annealing to 500 K (orange) and to 700 K (pink). (C) HREEL spectra of: (black trace) G*/Ni(111) immediately after ion bombardment (χ_{Ne^+} = 2.8 × 10^{14} Ne^+/cm^2). Notice that the broad loss around 150–172 meV is present also before dosing CO; (light blue to red traces) the same layer after subsequent cycles consisting of an exposure to 400 L at RT followed by annealing to 380 K; (top orange and green traces) G*/Ni(111) obtained after annealing freshly sputtered G/Ni(111) (χ_{Ne^+} = 3.2 × 10^{14} Ne^+/cm^2) to 500 K without CO exposure and after exposing to 400 L CO at RT. The different ratio of top and bridge CO depends on χ_{Ne^+}.

we can thus estimate a population of single double vacancies of ~4.5/1.5% respectively. Such estimate is compatible with the ratio of 5 : 2 for the population of single and di-vacancies taking into account an error of ±0.5% on the relative coverage.

(2) CO binds at the defected G*/Ni(111) surface as witnessed by the additional relevant energy losses. The relative intensity of the CO stretch mode for molecules at bridge and on-top sites depends on χ_{Ne^+}: initially the two sites are equally populated while with increasing sputtering dose the relative population observed for bare Ni(111) is approached.

The low intensity of the CO-stretch modes is due to the low concentration of vacancies in the G* layer and to the screening of the modes by the latter. Comparing the measured intensity of ν(CO) with the one reported for a coverage Θ_{CO} = 0.5 ML on Ni(111),[22] we estimate Θ_{CO} ~ 0.03 $ML_{Ni(111)}$ (1 $ML_{Ni(111)}$ = 1.86 × 10^{15} atoms per cm^2) for χ_{Ne^+} = 2.1 × 10^{14} Ne^+. In accord with this, XPS inspection shows only a very weak O 1s intensity around 531 eV (see inset of Fig. 3A), while the C 1s signal of CO expected around 286 eV[27] is too small to emerge from the much larger G-related component at 285 eV.[28] From comparison of the O 1s and C 1s intensities, we estimate a O/C ratio of ~2%, *i.e.* Θ_{CO} ~ 0.04 $ML_{Ni(111)}$, compatible with the coverage estimated by HREELS.

In the HREELS spectra the ratio of the two CO stretch peaks reflects the ratio of bridge/top sites for intercalated CO and does not provide any direct information about the morphology of the vacancy and different behaviours of single and double vacancies with respect to CO adsorption. Given the small CO coverage no conclusions could be derived from XPS either.

Although both estimates of defect density and of CO coverage may be affected by systematic errors, both the HREELS and the XPS analysis agree that the amount of defects introduced by ion bombardment in the G layer is only a few % of a ML. The distortion of the layer around the vacancies affects several neighbouring sites, causing a detectable shift of the C 1s peak. This is coherent with the STM information, which shows a modified density of states over an area significantly larger than the one corresponding to the single vacancy.

Fig. 4A shows the effect of annealing the CO/G*/Ni(111) sample. After flashing the sample above 400 K, all the CO-related losses disappear, while the broad energy loss feature around 169 meV survives, confirming that it loss is due to the distortion of C–C bonds in G*. The C 1s line remains unchanged up to T = 500 K (Fig. 3B) and it up-shifts towards the value of pristine G/Ni(111) when heating to 700 K. At the same T, the vibrational loss at 169 meV decreases in intensity. These observations indicate that the G sheet attaches again to the Ni substrate, although the initial state is not fully recovered: a shoulder at E_b = 283.4 eV is indeed present in the C 1s region and small losses at 90 and 62 meV are also visible. The C 1s component at 283.4 eV corresponds to nickel carbide[27] while the vibration at 62 meV is compatible with its vertical stretch (reported at 50 meV for C/Ni(100)[30] and at 59 meV for C/Ni(111) in presence of Na[20]).

For subsequent adsorption/annealing cycles (see Fig. 4C), a decreasing amount of CO adsorbs in the second and third uptake. In particular, on top sites are de-activated more rapidly than bridge sites.

If we anneal the sputtered surface to 500 K without pre-adsorbing CO, the vacancies remain reactive since thermal healing of vacancies occur at a definitely higher temperature (920 K according to Jacobson *et al.*[31]).

STM images of the annealed CO/G*/Ni(111) system (see Fig. 2C) confirm a significant modification of the surface morphology. Indeed, after annealing, the vacancies induced by sputtering are no longer detected, while the surface presents extended corrugated protrusions (in a quite disordered arrangement), the elongated shape of the ''scars'' suggests that, most likely, they derive from the healing of short line of single vacancies such as those apparent in Fig. 2C.

CO dissociation with reactive oxygen removal and healing of the original vacancy by the residual C atom was predicted by Wang and Pantelides for CO + NO reaction[7] and by Liu and Lee for CO + CO[9] on free standing graphene. If this were the relevant mechanism, then it should be active also for G* on Cu_{poly}, contrary to our experimental evidence. The theoretical calculations performed for free standing graphene are thus inadequate to describe the behaviour of supported graphene even for weakly interacting substrate as Cu. Probably the dangling bonds of the vacancies get saturated by binding to the substrate[18] which, therefore, plays an essential role in determining the reactivity of vacancies and their possible healing by chemical methods.

CO dissociation does not take place at regular bare Ni(111) sites. However, by introducing defects on a G/Ni(111) system, the ad-molecules are trapped between the metallic substrate and the G layer. Since only traces of oxygen remain when annealing to 450 K, it is reasonable that a Boudouard reaction, catalyzed by Ni, has occurred:[32,33]

$$2CO(ad) \xrightarrow[Ni]{} C + CO_2(g)$$

We thus conclude that vacancies allow CO adsorption in presence of a reactive substrate such as Ni. Intercalated CO molecules react when the system is annealed above 380 K leading to carbide formation, which can repair the vacancy and inhibit further CO adsorption in subsequent exposures.

Since vacancies are active only in presence of a reactive substrate and annealing does not restore the initial reactivity, we also conclude that neither single nor double vacancies can be the active sites responsible for the previously reported[13–15] sensing of CO. We suggest, therefore, that the effect must be due to defects, which are rare for high quality G films. Possible candidates could be Stone–Wales defects or edges of the graphene domains, for which the heat of adsorption is notoriously higher than at pristine G sites (thus explaining the need for annealing to 150 °C to regenerate the sensor). No healing of such defects upon CO adsorption can occur (thus explaining the reversibility of detection upon annealing[13] or at high temperature[15]). The small density of such sites for G/Ni(111), as well as for G/Cu_{poly}, and their lower heat of adsorption with respect to vacancy sites requires a relevant CO partial pressure to gain a significant transient CO coverage. This explains why no CO adsorption is observed under the UHV conditions of our experiment: a partial pressure of 10^{-6} mbar corresponds indeed to a relative concentration of 0.001 ppm at atmospheric pressure, *i.e.* to an expected equilibrium coverage of CO three orders of magnitude lower than the sensitivity of our spectroscopies.

Though negative, we believe that our results are of importance in view of the possible use of graphene based materials for applications in gas-sensing.

Furthermore, they can be extended and generalized to other supported 2D systems, for which defects have already been demonstrated to lower the barrier for dissociative adsorption.[34–37]

Acknowledgements

We acknowledge S. Agnoli (Università di Padova) for providing the G/Cu sample. We acknowledge A. Ambrosetti and P. L. Silvestrelli for scientific discussions. This work was founded by MIUR (projects PRIN GRAF 20105ZZTSE_003 and FIRB Futuro in Ricerca 2012 N. RBFR128BEC_004), Compagnia San Paolo and PRA 2013.

Notes and references

§ In the experiments reported in Fig. 1, no HREEL spectra of the defected G* layer have been recorded immediately after sputtering and prior to CO exposure. This was done to avoid unwanted CO contamination from the residual vacuum during the time necessary to record the HREEL spectrum.

1 B. F. Machado and P. Serp, *Catal. Sci. Technol.*, 2012, **2**, 54.
2 S. Sarkar, S. Niyogi, E. Bekyarova and R. C. Haddon, *Chem. Sci.*, 2011, **2**, 1326.
3 R. Mu, Q. Fu, L. Jin, L. Yu, G. Fang, D. Tan and X. Bao, *Angew. Chem., Int. Ed.*, 2012, **51**, 4856.
4 Y. Yao, Q. Fu, Y. Y. Zhang, X. Weng, H. Li, M. Chen, L. Jin, A. Dong, R. Mu, P. Jiang, L. Liu, H. Bluhm, Z. Liu, S. B. Zhang and X. Bao, *Proc. Natl. Acad. Sci. U. S. A.*, 2014, **111**, 17023.
5 E. Grånäs, J. Knudsen, U. A. Schröder, T. Gerber, C. Busse, M. A. Arman, K. Schulte, J. N. Andersen and T. Michely, *ACS Nano*, 2012, **6**, 9951.
6 O. Leenaerts, B. Partoens and F. Peeters, *Phys. Rev. B: Condens. Matter Mater. Phys.*, 2008, **77**, 125416.
7 B. Wang and S. T. Pantelides, *Phys. Rev. B: Condens. Matter Mater. Phys.*, 2011, **83**, 245403.
8 Y.-H. Zhang, Y. Chen, K.-G. Zhou, C. Liu, J. Zeng, H. Zhang and Y. Peng, *Nanotechnology*, 2009, **20**, 185504.
9 H. Liu and J. Y. Lee, *J. Phys. Chem. C*, 2012, **116**, 3034.
10 L. Tapasztó, G. Dobrik, P. Nemes-Incze, G. Vertesy, P. Lambin and L. P. Biró, *Phys. Rev. B: Condens. Matter Mater. Phys.*, 2008, **78**, 233407.
11 R. Martinazzo, S. Casolo and G. F. Tantardini, *Phys. Rev. B: Condens. Matter Mater. Phys.*, 2010, **81**, 245420.
12 R. Balog, B. Jørgensen, L. Nilsson, M. Andersen, E. Rienks, M. Bianchi, M. Fanetti, E. Lægsgaard, A. Baraldi, S. Lizzit, Z. Sljivancanin, F. Besenbacher, B. Hammer, T. G. Pedersen, P. Hofmann and L. Hornekær, *Nat. Mater.*, 2010, **9**, 315.
13 F. Schedin, A. K. Geim, S. V. Morozov, E. W. Hill, P. Blake, M. I. Katsnelson and K. S. Novoselov, *Nat. Mater.*, 2007, **6**, 652.
14 R. K. Joshi, H. Gomez, F. Alvi and A. Kumar, *J. Phys. Chem. C*, 2010, **114**, 6610.
15 E. Kayhan, R. M. Prasad, A. Gurlo, O. Yilmazoglu, J. Engstler, E. Ionescu, S. Yoon, A. Weidenkaff and J. J. Schneider, *Chem. – Eur. J.*, 2012, **18**, 14996.
16 M. Smerieri, E. Celasco, G. Carraro, A. Lusuan, J. Pal, G. Bracco, M. Rocca, L. Savio and L. Vattuone, *ChemCatChem*, 2015, **7**, 2328.
17 M. M. Ugeda, I. Brihuega, F. Hiebel, P. Mallet, J.-Y. Veuillen, J. M. Gómez-Rodríguez and F. Ynduráin, *Phys. Rev. B: Condens. Matter Mater. Phys.*, 2012, **85**, 121402.
18 M. M. Ugeda, D. Fernández-Torre, I. Brihuega, P. Pou, a. J. Martínez-Galera, R. Pérez and J. M. Gómez-Rodríguez, *Phys. Rev. Lett.*, 2011, **107**, 116803.

19 O. Lehtinen, J. Kotakoski, A. V. Krasheninnikov, A. Tolvanen, K. Nordlund and J. Keinonen, *Phys. Rev. B: Condens. Matter Mater. Phys.*, 2010, **81**, 153401.
20 A. Cupolillo, G. Chiarello, F. Veltri, D. Pacilè, M. Papagno, V. Formoso, E. Colavita and L. Papagno, *Chem. Phys. Lett.*, 2004, **398**, 118.
21 T. Aizawa, R. Souda, Y. Ishizawa, H. Hirano, T. Yamada, K. Tanaka and C. Oshima, *Surf. Sci.*, 1990, **237**, 194.
22 S. L. Tang, M. B. Lee, Q. Y. Yang, J. D. Beckerle and S. T. Ceyer, *J. Chem. Phys.*, 1986, **84**, 1876.
23 A. C. Ferrari and D. M. Basko, *Nat. Nanotechnol.*, 2013, **8**, 235.
24 A. Politano, M. Cattelan, D. W. Boukhvalov, D. Campi, A. Cupolillo, S. Agnoli, N. G. Apostol, P. Lacovig, S. Lizzit, D. Farias, G. Chiarello, G. Granozzi and R. Larciprete, *ACS Nano*, 2016, 6b00554.
25 A. Ambrosetti and P. L. Silvestrelli, *J. Chem. Phys.*, 2016, **144**, 111101.
26 F. Banhart, J. Kotakoski and A. V. Krasheninnikov, *ACS Nano*, 2011, **5**, 26.
27 M. Wei, Q. Fu, Y. Yang, W. Wei, E. J. Crumlin, H. Bluhm and X. Bao, *J. Phys. Chem. C*, 2015, 150526191240006.
28 W. Zhao, S. M. Kozlov, O. Höfert, K. Gotterbarm, M. P. A. Lorenz, F. Viñes, C. Papp, A. Görling and H.-P. Steinrück, *J. Phys. Chem. Lett.*, 2011, **2**, 759.
29 B. Borca, S. Barja, M. Garnica, M. Minniti, A. Politano, J. M. Rodriguez-García, J. J. Hinarejos, D. Farías, A. L. V. de Parga and R. Miranda, *New J. Phys.*, 2010, **12**, 093018.
30 M. Rocca, S. Lehwald, H. Ibach and T. S. Rahman, *Phys. Rev. B: Condens. Matter Mater. Phys.*, 1987, **35**, 9510.
31 P. Jacobson, B. Stöger, A. Garhofer, G. S. Parkinson, M. Schmid, R. Caudillo, F. Mittendorfer, J. Redinger and U. Diebold, *J. Phys. Chem. Lett.*, 2012, **3**, 136.
32 T. Osaki and T. Mori, *J. Catal.*, 2001, **204**, 89.
33 H. Nakano, J. Ogawa and J. Nakamura, *Surf. Sci.*, 2002, **514**, 256.
34 X. Wu, J. Yang, J. G. Hou and Q. Zhu, *J. Chem. Phys.*, 2006, **124**, 054706.
35 S. KC, R. C. Longo, R. M. Wallace and K. Cho, *J. Appl. Phys.*, 2015, **117**, 135301.
36 L. Nilsson, M. Andersen, R. Balog, E. Lægsgaard, P. Hofmann, F. Besenbacher, B. Hammer, I. Stensgaard and L. Hornekær, *ACS Nano*, 2012, **6**, 10258–10266.
37 D. L. Ma, Y. F. Zhang, M. X. Liu, Q. Q. Ji, T. Gao, T. Y. Zhang and Y. Z. F. Liu, *Nano Res.*, 2013, **6**, 671–678.